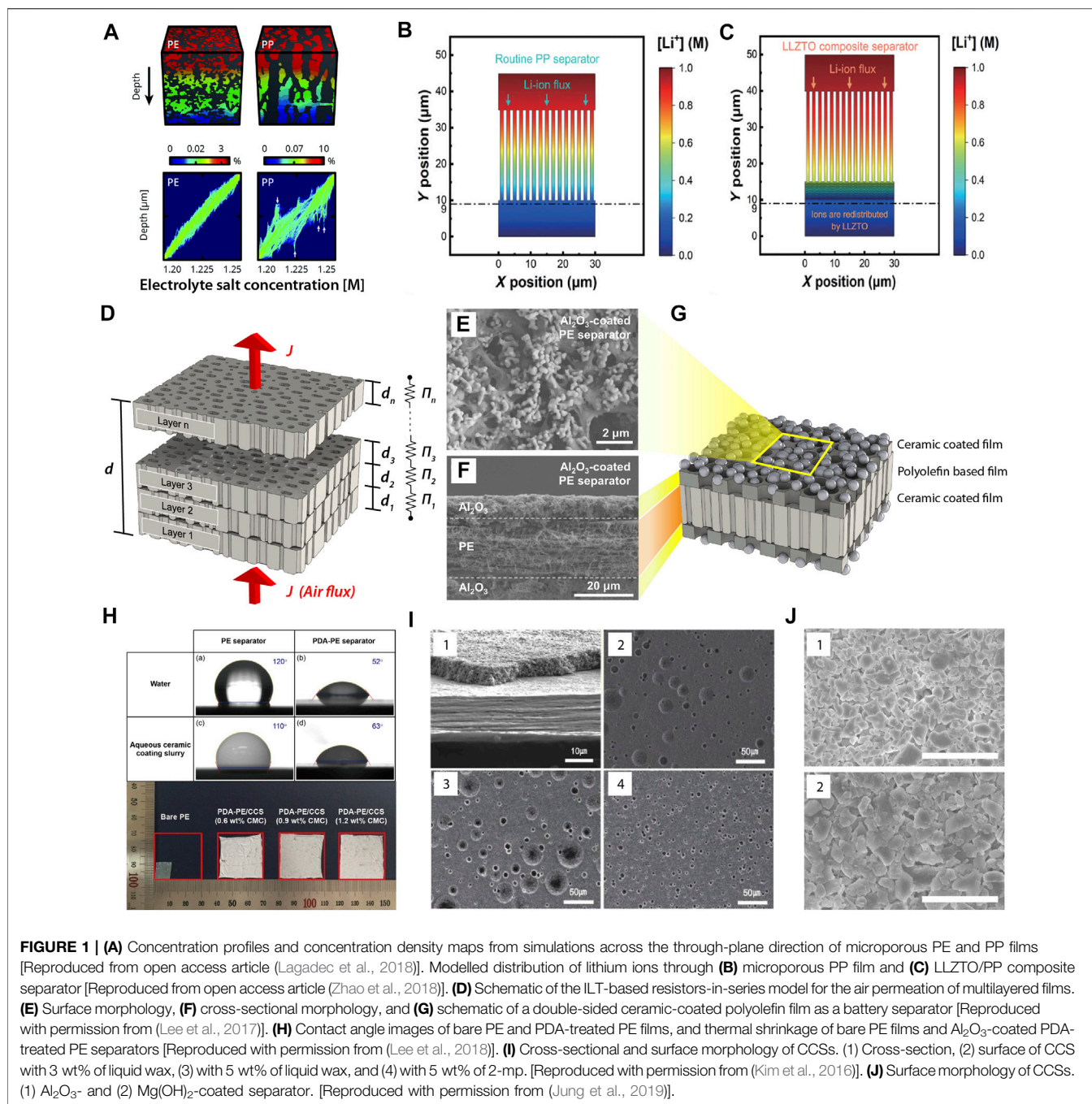# Estimating the Permeability of the Ceramic Coating on Lithium-Ion Battery Separators *via* the Ideal Laminate Theory

Sung Cik Mun[1]* and Jong Ho Won[2]*

[1]Future Technology Research Center, LG Chem, Seoul, South Korea, [2]Department of Chemistry, Kookmin University, Seoul, South Korea

In this study, a simple method for quantifying the porous nature based on the permeability of the thin ceramic coating on microporous polyolefin films used as separators in lithium-ion batteries is demonstrated. The air permeability of the ceramic coating was determined via the ideal laminate theory (ILT), which is widely accepted for multilayered films or well-defined laminates. This study mainly aims at introducing an ILT-based resistors-in-series model with the Gurley method and its potential applications in battery separators. We investigated a few previously reported examples of ceramic-coated separators to compare the air permeability of various ceramic coatings along with their base polyolefin films.

Keywords: lithium-ion battery, ceramic-coated separator, ideal laminate theory, Gurley method, permeability

INTRODUCTION

A lithium-ion battery separator is a major component crucial in ensuring the overall safety of the battery (Kim and Lee, 2016; Costa et al., 2019). This component serves as a physical barrier between the electrodes and a porous medium that allows the transmission of generated or consumed lithium ions during charging and discharging processes.(Arora and Zhang, 2004; Lee et al., 2014). Microporous polyolefin films [uniaxially stretched polypropylene (PP) and biaxially stretched polyethylene (PE)] have become popular in the separator industry owing to the uniformity of their micropores, chemical stability against electrolytes, high-oxidative decomposition potential versus Li/Li$^+$, excellent mechanical integrity during the assembly process in battery production when operated at normal operating temperatures, and a low cost (Mun and Won, 2021). However, these polyolefin films suffer from low thermal stability. A stretched polyolefin film shrinks at an elevated temperature as a result of the relaxation of polymer chains that were oriented under stress during the stretching process (Bourg et al., 2019). Above the melting temperatures, polyolefin films will lose their mechanical integrity such that the electrodes contact each other, leading to a short circuit (meltdown). PE films are more vulnerable to meltdown, because of their lower melting temperature (~ 135°C) than PP films (~ 165°C). In addition, the hydrophobic polyolefin films lack affinity for polar liquid electrolytes (Jeong et al., 2022). The wettability of a separator by electrolytes is critical in the internal resistance and ionic conductivity of lithium-ion batteries. The fast adsorption of electrolytes facilitates the electrolyte filling and wetting processes during the battery assembly, which are time-consuming steps in the manufacturing line (Davoodabadi et al., 2020). Several approaches have been suggested to overcome the poor wetting of polyolefin films. For example, the surface of PE films was modified by hydrophilic polydopamine (PDA) without compromising their morphological structure (Lee et al., 2018). The hydrophilic surface was also beneficial to the formation of a uniform ceramic

FIGURE 1 | (A) Concentration profiles and concentration density maps from simulations across the through-plane direction of microporous PE and PP films [Reproduced from open access article (Lagadec et al., 2018)]. Modelled distribution of lithium ions through **(B)** microporous PP film and **(C)** LLZTO/PP composite separator [Reproduced from open access article (Zhao et al., 2018)]. **(D)** Schematic of the ILT-based resistors-in-series model for the air permeation of multilayered films. **(E)** Surface morphology, **(F)** cross-sectional morphology, and **(G)** schematic of a double-sided ceramic-coated polyolefin film as a battery separator [Reproduced with permission from (Lee et al., 2017)]. **(H)** Contact angle images of bare PE and PDA-treated PE films, and thermal shrinkage of bare PE films and Al_2O_3-coated PDA-treated PE separators [Reproduced with permission from (Lee et al., 2018)]. **(I)** Cross-sectional and surface morphology of CCSs. (1) Cross-section, (2) surface of CCS with 3 wt% of liquid wax, (3) with 5 wt% of liquid wax, and (4) with 5 wt% of 2-mp. [Reproduced with permission from (Kim et al., 2016)]. **(J)** Surface morphology of CCSs. (1) Al_2O_3- and (2) $Mg(OH)_2$-coated separator. [Reproduced with permission from (Jung et al., 2019)].

layer on the separator surface. Besides the surface modification, the wettability of PE films toward electrolytes can be improved by an electrolyte additive such as a triblock polyether (Zheng et al., 2018).

Introducing a layer of hydrophilic ceramic particles at the surface can improve both low thermal stability and poor wettability of polyolefin films. It was demonstrated that ceramic particles improve the mechanical properties and dimensional stability of separators under thermal abuse (Shin and Kim, 2013; Lee et al., 2017). These ceramic particles also prevent the growth of lithium dendrites from the electrodes (Kim

and Lee, 2016; Costa et al., 2019) and improve abuse tolerance of bare polyolefin films toward nail penetration, impact, and inadvertent metal debris remaining from the manufacturing processes compared to bare polyolefin films (Alamgir et al., 2011). The aforementioned critical factors cause internal short-circuit failure or localized hotspots, thereby degrading the battery performance (Zhang et al., 2016). Improved wettability of polyolefin films by ceramic particles has also been reported in the literature. The PE films coated with Al_2O_3 and an acrylic binder exhibited higher electrolyte uptake and better wettability toward liquid electrolytes than

bare PE films (Kim et al., 2016). When compared with uncoated unilayer PE, unilayer PP, and trilayer PP/PE/PP films, Al_2O_3-coated PE films exhibited the fastest in-plane wetting behavior (Davoodabadi et al., 2020).

The ceramic-coated microporous polyolefin films have been commercialized for their applications in lithium-ion batteries. For example, LG Chem's safety-reinforced separator (SRS®) is a ceramic particle-coated polyolefin base film optimized for the lamination and stacking processes (Alamgir et al., 2011). Also, several manufacturers have developed ceramic-coated separators (CCSs) from a water-based slurry of ceramics. The ceramic coating layers comprise nano- or micro-sized ceramic particles and a polymeric binder, and occasionally involve a dispersant for ceramics in solvents. In typical commercial separators, a microporous ceramic layer provides a pathway for lithium ions. A porous structure filled with electrolytes between the positive and negative electrodes directly influences the cell performance associated with the mass transfer of lithium ions and the formation of lithium dendrite in lithium-ion batteries (Won et al., 2021). Understanding the microstructure of separators enables numerical simulations of the transport of lithium ions and the corresponding performance of lithium-ion batteries. Lagadec *et al.* introduced the concept of pore space connectivity, a parameter determined by topological or network-based analysis of separators, to predict cell performance and degradation with steady-state Fickian diffusion simulations (Lagadec et al., 2018). **Figure 1A** shows the difference in the concentration profiles and concentration density by the microstructures of PE and PP separators. In another research, simulations by finite element method predicted the roll of ion redistributors to eliminate dendrites by redistributing Li ions with Al-doped $Li_{6.75}La_3Zr_{1.75}Ta_{0.25}O_{12}$ (LLZTO) coated PP separators (**Figures 1B,C**) (Zhao et al., 2018). However, the numerical simulation with CCCs was rarely reported in the literature. Estimating the conduction of lithium ions through ceramic layers as well as the polyolefin base films is critical for achieving the target cell performance. To realize a suitable design for a ceramic-coated microporous polyolefin film as a separator, the porous structure of the ceramic layer should be understood.

CONCEPT FOR ESTIMATING THE PERMEABILITY WITH THE GURLEY METHOD

Measuring the air permeation of separators with or without a coating facilitates the indirect estimation of lithium-ion conduction via separators. Provided that the swelling of the polymeric binder caused by liquid electrolytes is negligible, the air permeation can be translated into lithium-ion conduction. The Gurley number is defined as the number of seconds required for 100 cm^3 of air to pass through 6.45 cm^2 of a given material at a pressure difference of 1.22 kPa, according to the T460 standards of the Technical Association of the Pulp and Paper Industry (TAPPI). It is a simple parameter used for estimating the mass transfer of air through a highly porous medium. The Gurley number is often referred to as "air permeability," which is an inaccurate interpretation. The Gurley number is inversely proportional to the

air permeance or air flux at a certain pressure difference. It should be noted that the Gurley number is dependent of the thickness, whereas the air permeability is a thickness-independent parameter (Arora and Zhang, 2004; Landesfeind et al., 2016).

In most cases, the porous properties of ceramic coatings could not be directly characterized using Gurley number, because the ceramic coating layer is too fragile to peel off from the microporous polyolefin film to obtain its freestanding form. Instead, the Gurley number of the entire separator (*i.e.*, the laminate of ceramic layers and polyolefin base film) has been used as the characterizing parameter mainly. This possibly affords misleading results when comparing the porous nature of ceramic coatings in different thicknesses. To reveal valid trends, the Gurley number with a known thickness of coating should be converted to the air permeability for comparing various ceramic coatings. This requires separation of the ceramic coating layer from the polyolefin base film for quantification. However, this type of quantification has rarely been reported. Therefore, in this study, we demonstrate a simple method based on the ideal laminate theory (ILT), which has been widely applied to multilayered gas barrier films, and present a few examples of its applications.

ILT FOR AIR PERMEATION IN MULTILAYERED FILMS

Consider a multilayered gas barrier film with a total thickness (d_n) between two arbitrary regions with a pressure difference (Δp), as depicted in **Figure 1D**. The corresponding permeability constant or permeability P is expressed as follows:

$$P = \Pi d_n = \frac{J}{\Delta p} d_n \qquad (1)$$

where Π is the permeance and J is the volumetric flux of the diffusing species. When materials with different permeabilities are stacked together to form a multilayered film. The permeance of the multilayered composite laminate can be calculated by adding the permeance of each layer i (analogous to "resistors in series") given as follows (Felts, 1991):

$$\Pi = \left(\sum_{i=1}^{n} \frac{1}{\Pi_i} \right)^{-1} \qquad (2)$$

This relationship is valid when the steady-state flux is the same in all layers and the permanent partial pressure is continuous at the boundary between the adjacent layers (Rossi and Nulman, 1993). The permeability (P) of the multilayered composite laminate is given as follows:

$$P = \left(\sum_{i=1}^{n} \frac{\Phi_i}{P_i} \right)^{-1} = \left(\sum_{i=1}^{n} \frac{d_i}{d_n P_i} \right)^{-1} \qquad (3)$$

where P_i is the permeability, d_i is the thickness, and ϕ_i is the volume fraction of a layer i. The Gurley number is inversely proportional to Π; therefore, the relationship between the Gurley number of the entire separator (t) and each layer i (t_i) can be expressed as follows:

TABLE 1 | Parameters of air permeation for microporous polyolefin base films, ceramic-coated polyolefin films and ceramic coating layers.

Parameters of Air Permeation for Microporous Polyolefin Base Films				
Ref	Type of polyolefin	Thickness (μm)	Gurley (s/100 ml)	Permeance (μm/s-Pa)	Permeability (μm²/s-Pa)
Lee et al. (2017)	PE	20	250	0.542	10.8
Lee et al. (2018)	PE/PP/PE tri-layer	23	425	0.319	7.3
Kim et al. (2016)	PE	20	285	0.475	9.5
Jung et al. (2019)	PE	14.1	184	0.736	10.4
Holtmann et al. (2016)	PE	12	172	0.79	9.5

Parameters of Air Permeation for Ceramic-Coated Polyolefin Films and Ceramic Coating Layers								
		Polyolefin with ceramic coating				Ceramic coating layer only		
Ref	Type of ceramics	Thickness (μm)	Gurley (s/100 ml)	Permeance (μm/s-Pa)	Permeability (μm²/s-Pa)	Thickness (μm)	Gurley (s/100 ml)	Permeance (μm/s-Pa)	Permeability (μm²/s-Pa)
Lee et al. (2017)	Unmilled Al_2O_3 (D_{50} = 3.75 μm)	35	358	0.378	13.2	15	108	1.26	18.8
Lee et al. (2017)	Jet-milled Al_2O_3 (D_{50} = 0.66 μm)	33	333	0.407	13.4	13	83	1.63	21.2
Lee et al. (2017)	Jet-milled Al_2O_3 (D_{50} = 0.55 μm)	32	326	0.416	13.3	12	76	1.78	21.4
Lee et al. (2017)	Jet-milled Al_2O_3 (D_{50} = 0.37 μm)	32	323	0.42	13.4	12	73	1.86	22.3
Lee et al. (2018)	Al_2O_3, 0.6 wt % CMC	27	300	0.452	12.2	7	15	9.03	63.2
Lee et al. (2018)	Al_2O_3, 0.9 wt % CMC	27	318	0.426	11.5	7	33	4.11	28.7
Lee et al. (2018)	Al_2O_3, 1.2 wt % CMC	27	333	0.407	11.0	7	48	2.82	19.8
Kim et al. (2016)	Al_2O_3, with no additive	16	215	0.631	10.1	4	43	3.14	12.6
Kim et al. (2016)	Al_2O_3, 1 wt% liquid wax	16	213	0.635	10.2	4	42	3.24	13.0
Kim et al. (2016)	Al_2O_3, 3 wt% liquid wax	16	225	0.604	9.7	4	53	2.56	10.2
Kim et al. (2016)	Al_2O_3, 5 wt% liquid wax	16	256	0.529	8.5	4	85	1.60	6.4
Kim et al. (2016)	Al_2O_3, 5 wt% 2-mp	16	208	0.653	10.4	4	36	3.76	15.1
Jung et al. (2019)	Al_2O_3	18.8	207	0.655	12.3	4.7	23	5.89	27.7
Jung et al. (2019)	$Mg(OH)_2$	18.5	234	0.579	10.7	4.4	50	2.71	11.9
Holtmann et al. (2016)	Boehmite, freestanding film	—	—	—	—	22	290	0.47	10.3

$$t = \sum_{i=1}^{n} t_i \qquad (4)$$

The permeability and permeance of each layer can be determined from Gurley numbers (in seconds per 100 ml) and the layer thickness as given by the following equations according to the T460 standards of TAPPI:

$$\Pi_i = \frac{135.5}{t_i}, P_i = \frac{135.5}{t_i} d_i \qquad (5)$$

where Π_i is expressed in micrometers per pascal second and P_i is expressed in square micrometers per pascal second. The

Equations 5 are valid for the multilayered composite laminate as well as an individual layer.

AIR PERMEABILITY OF CERAMIC COATING LAYERS ON SEPARATOR

The ILT has been widely used to estimate the permeability of constituting layers and has been validated for several systems, including silicon oxide-coated polymer films (Felts, 1991; Tropsha and Harvey, 1997; Roberts et al.,

2002), metallized polymer films (Jang et al., 2008), polymer films coated with layered double hydroxide nanosheets (Yu et al., 2020), and layer-by-layer assembled polymer composites with graphene oxide (Yang et al., 2013), graphene nanoplatelets (Mun et al., 2017), and nanoclay (Priolo et al., 2010). In this study, air permeation parameters of several ceramic coatings of different constituents with various thicknesses on polyolefin base films were estimated using the ILT model. To apply the ILT model for battery separators, the thicknesses and Gurley numbers of the entire separator and the base film should be given. In addition, a well-defined thickness will allow accurate estimation of air permeability for ceramic coating layers. Ceramic coating on a polyolefilm base film can be double sided or single sided. In most cases, the ceramic coating is unilayer. If the porous structure is the same in both layers of the double-sided coating, we can assume that the permeability of the layers is the same. We investigated a few examples for comparing the permeability of various ceramic coating layers reported (**Table 1**). The parameters of air permeation for polyolefin base films were also listed for comparison.

In a previous study, jet-milled α-Al_2O_3 particles were dip coated on a 20-μm-thick PE film from an acetone-based slurry comprising α-Al_2O_3 particles and poly (vinylidene fluoride-co-hexafluoropropylene) (50/50 by weight) (Lee et al., 2017). **Figures 1E–G** depict a typical morphology of a double-sided ceramic-coated polyolefin base film. The ceramic layer with a thickness of 12–15 μm reduced the thermal shrinkage and improved the melt integrity of a pristine PE film without adversely affecting the rate capability and cycling performance. Furthermore, they investigated the effect of Al_2O_3 particle size on the properties of coated separators. The Gurley number of the separator with various jet-milled Al_2O_3 particles (D_{50} = 0.37–0.66 μm) was lower than that of the separator with unmilled large Al_2O_3 particles (D_{50} = 3.75 μm). However, these Gurley numbers were associated with different coating thicknesses. **Table 1** summarizes the parameters associated with air permeation for the ceramic-coated polyolefin film and ceramic coating layers only. The estimated permeability of ceramic coating layers can be used to characterize their intrinsic porous natures. Considering the experimental errors, the change in permeability induced by the difference in sizes of the jet-milled Al_2O_3 particles was marginal.

Although poly (vinylidene fluoride) (PVdF) and its copolymers are commonly used in battery applications as binders, the application of these materials in an aqueous process is limited by their insolubility in water. Water-soluble binders attracted considerable interest as a replacement to organic solvents with cost-effective and eco-friendly aqueous slurries. For example, Al_2O_3 particles were coated on PDA-treated PE films developed using a water-based slurry with carboxyl methyl cellulose (CMC) as a binder (Lee et al., 2018). The PDA treatment improved the wettability of aqueous ceramic coating slurry toward PE films, which assisted the formation of uniform ceramic coating on the PE films (**Figure 1H**). The

ceramic coating layer with a thickness of 7 μm did not deteriorate the lithium ion conductance and electrochemical properties, but significantly improved the thermal stability at 140°C for 1 h (**Figure 1H**). High loading levels of binder improved the interfacial adhesion between the ceramic coating layer and a 20-μm-thick PE base film. However, as the polymeric binder content increased, the permeability gradually decreased, indicating the high tortuosity or the low porosity of the separators. **Table 1** shows that the air permeability considerably changed with slight changes in the binder content. A binder content of 0.6 wt.% was effective in improving thermal stability, whereas content of 0.9 and 1.2 wt.% yielded better cell resistance and discharge capacity. Owing to the similar electrolyte uptakes (~ 120%) regardless of binder content, a more permeable ceramic coating yielded a higher ionic conductivity than a less permeable coating. The authors fabricated a ceramic coating with a permeability of up to 63.2 $μm^2$/s-Pa.

In another study, an aqueous acrylic emulsion binder and Al_2O_3 particles were used to form a 4-μm-thick ceramic coating on one side of a bare PE film (Kim et al., 2016). The ceramic coating improved the thermal stability, electrolyte uptake, puncture strength, ionic conductivity, and rate capability of the PE film. A small amount of liquid wax or 2-methyl pentane (2-mp) was added to the slurry to reduce moisture adsorption, which negatively affects battery performance. The CCSs have unique surface morphology with craters on their surfaces due to the oil additives (**Figure 1I**). Despite the beneficial aspects of the wax, the Gurley number increased with the liquid wax content. However, the incorporation of volatile 2-mp into the aqueous slurry did not increase the Gurley number as much as the liquid wax because 2-mp evaporated during the drying procedure. The estimated permeability of each coating is listed in **Table 1**.

The choice of ceramics for separator coating is not limited to Al_2O_3 particles. Two types of non-aqueous CCSs, based on Al_2O_3 and $Mg(OH)_2$, were manufactured at a pilot (Jung et al., 2019). The surface micrographs confirmed that both ceramic particles are similar in lateral size and closely packed in the coated layer (**Figure 1J**). Although both coated separators exhibited almost no thermal shrinkage at 200°C, and good wettability towards electrolytes, $Mg(OH)_2$-coated separators were more flexible and tough than Al_2O_3-coated separators. This difference in mechanical properties was reflected in nail penetration tests more than electrochemical performance. However, it should be noted that the permeability of Al_2O_3 coating was more than twice as high as $Mg(OH)_2$ coating (**Table 1**). This might be one of the reasons that the ionic conductivity of $Mg(OH)_2$-coated separator was lower than Al_2O_3-coated separator with a similar coating thickness.

Holtmann et al. prepared a freestanding ceramic separator based on surface-functionalized boehmite nanoparticles with PVdF as a binder (Holtmann et al., 2016). Unlike previous cases, the Gurley number was directly measured from the freestanding form with a thickness of 22 μm. The permeability (10.3 $μm^2$/s-Pa) was comparable to that of the polyolefin base films but lower than that of the typical ceramic coating layers (**Table 1**). In addition, the tensile strength (6.3–6.5 MPa) and elongation at break (16–21%) of the film were considerably lower than those of

the stretched polyolefin films (Mun and Won, 2021). This indicates the technical difficulty of fabricating freestanding ceramic separators with excellent mechanical properties.

CONCLUSION

In this study, we investigated the application of the ILT model to CCSs used in lithium-ion batteries. By separating the permeability of the ceramic coating layers from that of the polyolefin base films, the intrinsic porous property of ceramic layers determined in each study can be compared. Based on the results of this study, a simple tool may be obtained for the elaborate design of functional coatings or additional layers on substrates for a multilayered microporous medium.

REFERENCES

Alamgir, M., Ketkar, S., and Yoo, K. (2011). "Recent Progresses of LG Chem's Large-Format Li Ion Polymer Batteries," in 2011 IEEE Power and Energy Society General Meeting, Detroit, MI, USA, July 2011, 1–4. doi:10.1109/PES.2011.6039774

Arora, P., and Zhang, Z. (2004). Battery Separators. *Chem. Rev.* 104, 4419–4462. doi:10.1021/cr020738u

Bourg, V., Ienny, P., Caro-Bretelle, A. S., Le Moigne, N., Guillard, V., and Bergeret, A. (2019). Modeling of Internal Residual Stress in Linear and Branched Polyethylene Films during Cast Film Extrusion: Towards a Prediction of Heat-Shrinkability. *J. Mater. Process. Technol.* 271, 599–608. doi:10.1016/j.jmatprotec.2019.04.002

Costa, C. M., Lee, Y.-H., Kim, J.-H., Lee, S.-Y., and Lanceros-Méndez, S. (2019). Recent Advances on Separator Membranes for Lithium-Ion Battery Applications: From Porous Membranes to Solid Electrolytes. *Energy Storage Mater.* 22, 346–375. doi:10.1016/j.ensm.2019.07.024

Davoodabadi, A., Jin, C., Wood, D. L., III, Singler, T. J., and Li, J. (2020). On Electrolyte Wetting through Lithium-Ion Battery Separators. *Extreme Mech. Lett.* 40, 100960. doi:10.1016/j.eml.2020.100960

Felts, J. T. (1991). "Thickness Effects on Thin Film Gas Barriers : Silicon-Based Coatings," in Society of Vacuum Coaters; 34th Annual Technical Conference Proceedings, 99–104.

Holtmann, J., Schäfer, M., Niemöller, A., Winter, M., Lex-Balducci, A., and Obeidi, S. (2016). Boehmite-based Ceramic Separator for Lithium-Ion Batteries. *J. Appl. Electrochem.* 46, 69–76. doi:10.1007/s10800-015-0895-z

Jang, C., Cho, Y.-R., and Han, B. (2008). Ideal Laminate Theory for Water Transport Analysis of Metal-Coated Polymer Films. *Appl. Phys. Lett.* 93, 133307. doi:10.1063/1.2996018

Jeong, W., Kang, J., Lim, S. Y., Ahn, H., Kim, H. M., Won, J. H., et al. (2022). Spontaneously Induced Hierarchical Structure by Surface Energy in Novel Conjugated Polymer-Based Ultrafast-Response Organic Photodetectors. *Adv. Opt. Mater.* 10, 2102607. doi:10.1002/adom.202102607

Jung, B., Lee, B., Jeong, Y.-C., Lee, J., Yang, S. R., Kim, H., et al. (2019). Thermally Stable Non-aqueous Ceramic-Coated Separators with Enhanced Nail Penetration Performance. *J. Power Sources* 427, 271–282. doi:10.1016/j.jpowsour.2019.04.046

Kim, J.-H., Lee, S.-Y., and Lee, S.-Y. (2016). Current Status and Future Research Directions of Separator Membranes for Lithium-Ion Rechargeable Batteries. *Membr. J.* 26, 337–350. doi:10.14579/membrane_journal.2016.26.5.337

Kim, S. W., Ryou, M.-H., Lee, Y. M., and Cho, K. Y. (2016). Effect of Liquid Oil Additive on Lithium-Ion Battery Ceramic Composite Separator Prepared with an Aqueous Coating Solution. *J. Alloys Compd.* 675, 341–347. doi:10.1016/j.jallcom.2016.03.135

Lagadec, M. F., Zahn, R., Müller, S., and Wood, V. (2018). Topological and Network Analysis of Lithium Ion Battery Components: The Importance of Pore Space Connectivity for Cell Operation. *Energy Environ. Sci.* 11, 3194–3200. doi:10.1039/c8ee00875b

Landesfeind, J., Hattendorff, J., Ehrl, A., Wall, W. A., and Gasteiger, H. A. (2016). Tortuosity Determination of Battery Electrodes and Separators by Impedance Spectroscopy. *J. Electrochem. Soc.* 163, A1373–A1387. doi:10.1149/2.1141607jes

Lee, D.-W., Lee, S.-H., Kim, Y.-N., and Oh, J.-M. (2017). Preparation of a High-Purity Ultrafine α-Al2O3 Powder and Characterization of an Al2O3-Coated PE Separator for Lithium-Ion Batteries. *Powder Technol.* 320, 125–132. doi:10.1016/j.powtec.2017.07.027

Lee, H., Jeon, H., Gong, S., Ryou, M.-H., and Lee, Y. M. (2018). A Facile Method to Enhance the Uniformity and Adhesion Properties of Water-Based Ceramic Coating Layers on Hydrophobic Polyethylene Separators. *Appl. Surf. Sci.* 427, 139–146. doi:10.1016/j.apsusc.2017.07.276

Lee, H., Yanilmaz, M., Toprakci, O., Fu, K., and Zhang, X. (2014). A Review of Recent Developments in Membrane Separators for Rechargeable Lithium-Ion Batteries. *Energy Environ. Sci.* 7, 3857–3886. doi:10.1039/C4EE01432D

Mun, S. C., Park, J. J., Park, Y. T., Kim, D. Y., Lee, S. W., Cobos, M., et al. (2017). High Electrical Conductivity and Oxygen Barrier Property of Polymer-Stabilized Graphene Thin Films. *Carbon* 125, 492–499. doi:10.1016/j.carbon.2017.09.088

Mun, S. C., and Won, J. H. (2021). Manufacturing Processes of Microporous Polyolefin Separators for Lithium-Ion Batteries and Correlations between Mechanical and Physical Properties. *Crystals* 11, 1013. doi:10.3390/cryst11091013

Priolo, M. A., Gamboa, D., Holder, K. M., and Grunlan, J. C. (2010). Super Gas Barrier of Transparent Polymer–Clay Multilayer Ultrathin Films. *Nano Lett.* 10, 4970–4974. doi:10.1021/nl103047k

Roberts, A. P., Henry, B. M., Sutton, A. P., Grovenor, C. R. M., Briggs, G. A. D., Miyamoto, T., et al. (2002). Gas Permeation in Silicon-Oxide/polymer (SiOx/PET) Barrier Films: Role of the Oxide Lattice, Nano-Defects and Macro-Defects. *J. Membr. Sci.* 208, 75–88. doi:10.1016/s0376-7388(02)00178-3

Rossi, G., and Nulman, M. (1993). Effect of Local Flaws in Polymeric Permeation Reducing Barriers. *J. Appl. Phys.* 74, 5471–5475. doi:10.1063/1.354227

Shin, W.-K., and Kim, D.-W. (2013). High Performance Ceramic-Coated Separators Prepared with Lithium Ion-Containing SiO2 Particles for Lithium-Ion Batteries. *J. Power Sources* 226, 54–60. doi:10.1016/j.jpowsour.2012.10.082

Tropsha, Y. G., and Harvey, N. G. (1997). Activated Rate Theory Treatment of Oxygen and Water Transport through Silicon Oxide/poly(ethylene Terephthalate) Composite Barrier Structures. *J. Phys. Chem. B* 101, 2259–2266. doi:10.1021/jp9629856

Won, J. H., Kim, M. K., and Jeong, H. M. (2021). Porous Polymer Thin Film Encapsulated Sulfur Nanoparticles on Graphene via Partial Evaporation for High-Performance Lithium-Sulfur Batteries. *Appl. Surf. Sci.* 547, 149199. doi:10.1016/j.apsusc.2021.149199

AUTHOR CONTRIBUTIONS

Conceptualization, SM and JW; writing-original draft preparation, SM; writing-review and editing, JW; funding acquisition, JW. All authors have read and agreed to the published version of the manuscript.

FUNDING

Yang, Y.-H., Bolling, L., Priolo, M. A., and Grunlan, J. C. (2013). Super Gas Barrier and Selectivity of Graphene Oxide-Polymer Multilayer Thin Films. *Adv. Mat.* 25, 503–508. doi:10.1002/adma.201202951

Yu, J., Buffet, J.-C., and O'Hare, D. (2020). Aspect Ratio Control of Layered Double Hydroxide Nanosheets and Their Application for High Oxygen Barrier Coating in Flexible Food Packaging. *ACS Appl. Mat. Interfaces* 12, 10973–10982. doi:10.1021/acsami.9b21986

Zhang, X., Sahraei, E., and Wang, K. (2016). Li-ion Battery Separators, Mechanical Integrity and Failure Mechanisms Leading to Soft and Hard Internal Shorts. *Sci. Rep.* 6, 32578. doi:10.1038/srep32578

Zhao, C.-Z., Chen, P.-Y., Zhang, R., Chen, X., Li, B.-Q., Zhang, X.-Q., et al. (2018). An Ion Redistributor for Dendrite-free Lithium Metal Anodes. *Sci. Adv.* 4, eaat3446. doi:10.1126/sciadv.aat3446

Zheng, H., Xie, Y., Xiang, H., Shi, P., Liang, X., and Xu, W. (2018). A Bifunctional Electrolyte Additive for Separator Wetting and Dendrite Suppression in Lithium Metal Batteries. *Electrochimica Acta* 270, 62–69. doi:10.1016/j.electacta.2018.03.089